Green Chemistry

Accepted Manuscript

This article can be cited before page numbers have been issued, to do this please use: Y. Li, S. Leow, A. C. Fedders, B. K. Sharma, J. Guest and T. J. Strathmann, *Green Chem.*, 2017, DOI: 10.1039/C6GC03294J.

ROYAL SOCIETY OF CHEMISTRY

rsc.li/green-chem

Green Chemistry

View Article Online
DOI: 10.1039/C6GC03294J

PAPER

Quantitative multiphase model for hydrothermal liquefaction of algal biomass†

Received 00th January 20xx,
Accepted 00th January 20xx

DOI: 10.1039/x0xx00000x

www.rsc.org/greenchem

Yalin Li,[a] Shijie Leow,[a,b] Anna C. Fedders,[b] Brajendra K. Sharma,[c] Jeremy S. Guest[b] and Timothy J. Strathmann*[a,d]

Optimized incorporation of hydrothermal liquefaction (HTL, reaction in water at elevated temperature and pressure) within an integrated biorefinery requires accurate models to predict the quantity and quality of all HTL products. Existing models primarily focus on biocrude product yields with limited consideration for biocrude quality and aqueous, gas, and biochar co-products, and have not been validated with an extensive collection of feedstocks. In this study, HTL experiments (300 °C, 30 min) were conducted using 24 different batches of microalgae feedstocks with distinctive feedstock properties, which resulted in a wide range of biocrude (21.3 – 54.3 dry weight basis, dw%), aqueous (4.6 – 31.2 dw%), gas (7.1 – 35.6 dw%), and biochar (1.3 – 35.0 dw%) yields. Based on these results, a multiphase component additivity (MCA) model was introduced to predict yields and characteristics of the HTL biocrude product and aqueous, gas, and biochar co-products, with only feedstock biochemical (lipid, protein, carbohydrate, and ash) and elemental (C/H/N) composition as model inputs. Biochemical components were determined to distribute across biocrude product/HTL co-products as follows: lipids to biocrude; protein to biocrude > aqueous > gas; carbohydrates to gas ≈ biochar > biocrude; and ash to aqueous > biochar. Modeled quality indicators included biocrude C/H/N contents, higher heating value (HHV), and energy recovery (ER); aqueous total organic carbon (TOC) and total nitrogen (TN) contents; and biochar carbon content. The model was validated with HTL data from the literature, the potential to expand the application of this modeling framework to include waste biosolids (*e.g.*, wastewater sludge, manure) was explored, and future research needs for industrial application were identified. Ultimately, the MCA model represents a critical step towards the integration of cultivation models with downstream HTL and biorefinery operations to enable system-level optimization, valorization of co-product streams (*e.g.*, through catalytic hydrothermal gasification and nutrient recovery), and the navigation of tradeoffs across the value chain.

1 Introduction

In recent years, biomass-derived renewable fuels have received increasing attention from government and commercial entities. Among potential biomass feedstocks, microalgae have a number of favorable properties that show promise for large-scale biofuel production, including high productivity, cultivation flexibility (*e.g.*, use of non-arable land and a wide variety of water sources), and potential to be cultivated to various biochemical compositions.[1–3] Hydrothermal liquefaction (HTL) applies elevated temperature and pressure (200 – 350 °C, 5 – 20 MPa) to promote biomass decomposition and reformation in water, forming an energy-dense, self-separating biocrude oil product as well as aqueous, gas, and biochar co-products.[4] With the elimination of energy-intensive drying steps, HTL has attracted growing interests as a downstream biorefinery technology for processing wet algal biomass.[5–7] A recent life cycle assessment (LCA) of algal HTL showed a higher energy return on investment than conventional biofuel processing (*e.g.*, corn ethanol, cellulosic ethanol, soybean biodiesel), but the current costs of HTL-derived algal fuels remain well above those of fossil fuels.[2,8–10] Therefore, improvements in process integration are needed to lower biofuel production costs, requiring an integrated modeling platform to connect upstream cultivation decisions to downstream conversion outcomes. As a crucial step towards this objective, quantitative relationships connecting feedstock properties to HTL products (both the biocrude product and co-products) are needed.

Biller and Ross[11] first introduced a linear "component additivity" approach to predict biocrude product yields, formulating HTL biocrude yields (Y_{Bio}) for algal biomass as the summation of yields from lipid (L), protein (P), and carbohydrate (C) components in the cellular biomass:

$$Y_{Bio} = k_L \times L + k_P \times P + k_C \times C \quad (1)$$

where k_L, k_P, and k_C are coefficients for the conversion efficiency of individual biochemical components to biocrude products. Instead of using algal biomass, these authors and others[12]

[a] Colorado School of Mines, Department of Civil and Environmental Engineering, Golden, CO 80401, USA.
[b] University of Illinois at Urbana-Champaign, Department of Civil and Environmental Engineering, Urbana, IL 61801, USA.
[c] University of Illinois at Urbana-Champaign, Illinois Sustainable Technology Center, Champaign, IL 61820, USA.
[d] National Renewable Energy Laboratory, Golden, CO 80401, USA.
* Corresponding author, E-mail: strthmnn@mines.edu, Phone: +1.303.384.2226
† Electronic Supplementary Information (ESI) available: Feedstock acquisition, experimental methods and results, statistical analyses, cited literature data, and additional supporting figures. See DOI: 10.1039/x0xx00000x

calibrated the model coefficients using reference compounds of each component. More recently, Leow *et al.* re-calibrated and improved the accuracy of the additivity model using HTL measurements from the microalgae species *Nannochloropsis oculata*.[4] However, all current component additivity models remain constrained to predicting only biocrude yields. Meanwhile, Valdez and co-workers established a reaction network model addressing HTL kinetics at varying reaction conditions.[13–15] Furthermore, more recent studies have been conducted to examine the impacts of kinetics factors (*e.g.*, heating rate) on HTL reactions, and a new reaction network model has been proposed.[16,17] These models are able to predict time dependent yields of all HTL products, but also indicate that the yields will reach steady state values upon completion of the reactions (typically within 30 min in small tube reactors), providing additional justification for the application of additivity models. However, all above models are unable to predict characteristics of the individual HTL products (*e.g.*, elemental composition). Leow *et al.* partially addressed this by introducing a new fatty acid (FA) conservation model that predicts both the yields and elemental (C/H/N/O) contents of biocrude product by separately considering HTL conversion of fatty acid and non-fatty acid fractions of the algal biomass, but more extensive experiments are required to determine the composition of FA and non-FA fractions.[4]

Though these models have significantly advanced our predictive power, limitations on HTL co-product predictions need to be addressed since they can represent more than 40% of the feedstock carbon and 70% of the feedstock nutrients.[18] Only with information on both yields and compositions of all HTL products can developers effectively lower the minimum fuel selling price (MFSP) and mitigate environmental impacts of HTL-derived fuels through co-product valorization and integrated resource (carbon, nitrogen, water, *etc.*) management.[10,18] Beyond algae, other organic waste streams – such as anaerobic sludge,[19] sewage sludge,[20,21] and animal manure[19,22] – have also been identified as attractive HTL feedstock candidates, and these waste streams represent a considerable untapped source of energy. Currently, 7.2 million dry tons of sewage sludge are generated in the U.S. annually,[23] but only 60% of them is diverted to beneficial use,[19] and the cost can be up to $800 per dry ton.[24] Furthermore, U.S. agricultural industries produce approximately 250 million dry tons of fecal material each year, which has energy content equivalent to 21 billion gallons of gasoline,[25] or 8% of the petroleum consumed in the U.S. in 2015.[26] HTL has been promoted as a promising technology for valorizing these waste streams,[19,22] but comprehensive predictive models are required to evaluate the biofuel production potential and improve recovery efficiency through this technique.

Therefore, new HTL models must be developed to predict both yields as well as characteristics of all HTL products, and encompass feedstocks beyond microalgae. This contribution describes the formulation, calibration, and validation of a new multiphase component additivity (MCA) model for HTL processing of algal biomass. The model was developed using HTL experimental data (300 °C, 30 min) generated from 24 different feedstocks (12 batches of microalgae with their defatted analogues). It links yields and elemental composition of HTL products to readily measurable biochemical properties and major elemental composition of feedstocks. Validated by external data of microalgae and waste biosolids, the model provides mechanistic insight into the partitioning of elements between HTL products, tradeoffs between biocrude yields and upgrading requirements, and potential for co-product utilization.

2 Results and discussion

2.1 HTL multiphase products yields

In this study, 24 batches of microalgae with distinctive biochemical and elemental compositions (0 – 43.0 dw% lipids, 11.4 – 69.8 dw% proteins, 10.0 – 63.6 dw% carbohydrates, and 2.0 – 13.1 dw% ash, Figure S1 in the ESI†, dw% is on dry weight basis) were used as feedstocks for HTL conversion experiments (300 °C for 30 min), and the collected data were used for model development and calibration. Individual product yields varied extensively with yields of biocrude product ranging from 21.3 to 54.3 dw%, aqueous co-product from 4.6 to 31.2 dw% (measured as total dissolved solids, TDS), gas co-product from 7.1 to 35.6 dw%, and biochar co-product from 1.3 to 35.0 dw% (**Figure 1**, Tables S1 and S2 in the ESI†).

Compositional trends demonstrate that increasing biocrude yield is accompanied by increasing feedstock lipid content (**Figure 1a**, left), in agreement with predictions from existing biocrude component additivity models.[4,11,12] Increasing aqueous co-product yield is associated with increasing feedstock protein content (**Figure 1b**, left). Both gas and biochar co-product yields (**Figure 1c – d**, left) show similar trends, with their yields increasing in association with increasing carbohydrate content. The observed trends are consistent with statistical analysis, where the Pearson Correlation Coefficients (PCC, Table S4 in the ESI†) between feedstock components and products show that biocrude yield correlates most strongly with feedstock lipid content (PCC = 0.64), aqueous yield with protein content (PCC = 0.82), and gas as well as biochar yields with carbohydrate content (PCC = 0.89 and 0.80, respectively). Noticeably, aqueous yield also appears to be positively correlated with feedstock ash content with a large PCC of 0.76 (Figure S2 in the ESI†), implying contribution of ash component in the biomass to the aqueous co-product. Therefore, yield of all four HTL products is formulated as:

$$Y_i = \sum Y_{ij} = \sum k_{ij} \times j = k_{iL} \times L + k_{iP} \times P + k_{iC} \times C + k_{iA} \times A \quad (2)$$

View Article Online
DOI: 10.1039/C6GC03294J

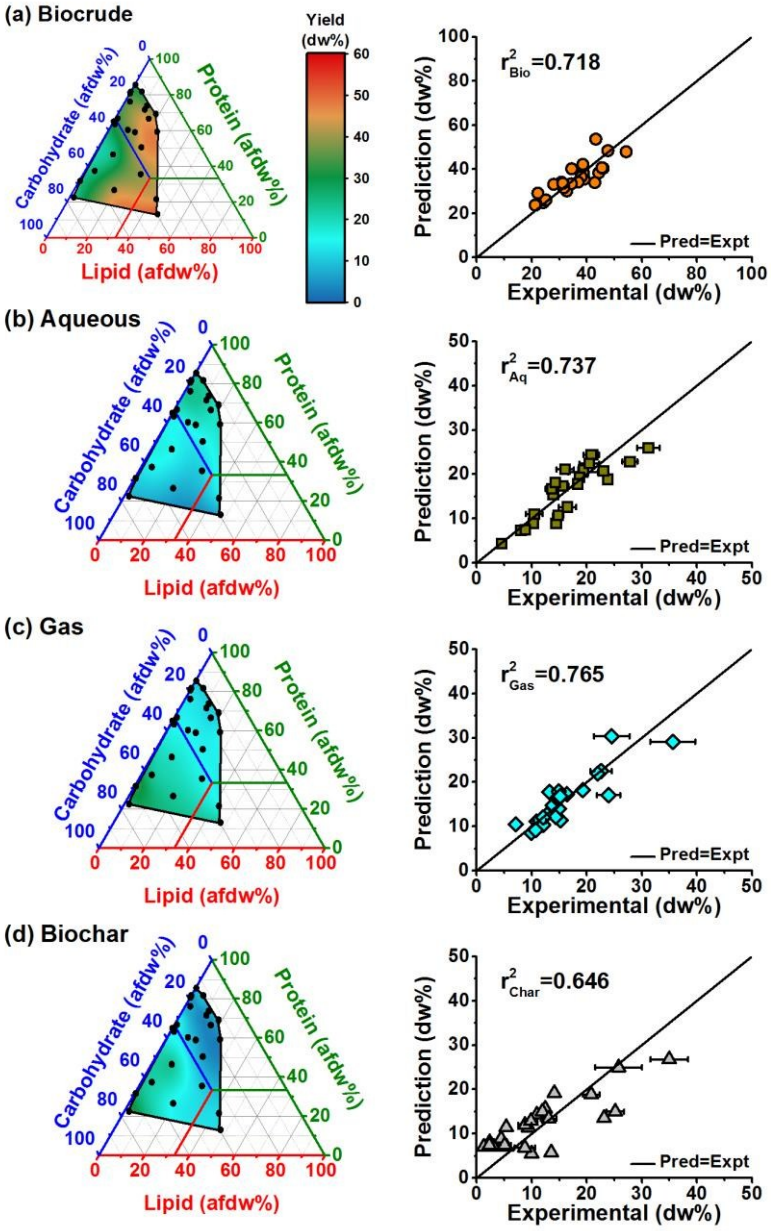

Figure 1 Experimental HTL yields and MCA predictions for (a) biocrude, (b) aqueous, (c) gas, and (d) biochar products. Left column: relationships between feedstock volatile (non-ash, corrected to 100 afdw%, ash free dry weight) composition and measured HTL yields (dw%). Discrete points represent data used to generate the contour plots by interpolation, and blank areas fall outside of the feedstock composition range examined. Right column: predictions versus experimental results for calibration data (from this study). R^2 values are relative to the 1:1 lines. Error bars represent max/min values measured in duplicate experiments (not shown if smaller than the symbol size). Detailed HTL product data provided in Table S2 in the ESI†.

During HTL, a fixed fraction (k_{ij}, **Table 1**) of each biomass component j is assumed to be converted to a particular product i, with the total yield of that product (Y_i) being a linear summation of individual component yields (Y_{ij}). In addition to the lipid (L), protein (P), and carbohydrate (C) components, ash (A) is added as a fourth component to account for inorganic constituents contributing to aqueous and biochar co-products, which cannot be neglected, especially for marine,[27] wild,[28] or wastewater[29] species with high ash contents. Details on regression methods used for model calibration are provided in Section 4.3. All product yields can be predicted (**Figure 1**, right column) using eq 2 and the corresponding coefficients listed in **Table 1**. Generally, predictions fall evenly around the 1:1 correlation lines, and calculated r^2 values are relatively large, ranging from 0.646 (biochar) to 0.765 (gas). Therefore, the

observed trends and our proposal of the MCA model for yield prediction were internally validated.

Table 1 MCA model coefficients for HTL product yields[a]

Phase	L	P	C	A
Biocrude	0.85 (±0.16)[b]	0.45 (±0.06)	0.22 (±0.10)	-[c]
Aqueous	-	0.24 (±0.09)	-	0.86 (±0.63)
Gas	-	0.07 (±0.04)	0.46 (±0.06)	-
Biochar	-	-	0.41 (±0.10)	0.18 (±0.43)

[a] Final matrix of the MCA model for yield predictions (eq 2), calibrated with experimental data from this study (96 data points and 9 adjustable coefficients) using Solver and Regression programs in Microsoft® Excel 2016 Analysis Toolpak.

[b] Uncertainties provided at the 95% confidence level.

[c] - Denotes coefficients excluded from model fitting.

Coefficients for biocrude products formation reveal a trend similar to those reported in previous calibrations of biocrude-only component additivity models.[4,11,12] That is, lipids have the highest conversion coefficient (0.85), followed by proteins with a moderate conversion efficiency (0.45), and a lower coefficient (0.22) for carbohydrates. Compared with the biocrude additivity model presented by Leow *et al.* (eq S1 in the ESI†),[4] coefficients for protein-to-biocrude (0.42) and carbohydrate-to-biocrude (0.17) conversion are close to those determined here, and the associated uncertainty for carbohydrate conversion has been substantially reduced (±0.10 versus ±0.35 in Leow *et al.*) due to the much wider range of feedstock carbohydrate contents in the present calibration dataset. However, the lipid-to-biocrude conversion coefficient here (0.85) is smaller than the previously reported value (0.97). The difference is mainly attributed to the differences in lipid composition of microalgae species used in these two studies. The Folch method[30] (used for lipid quantification in both studies) determines the gross lipid contents containing both polar and neutral fractions. Studies have shown that while the fatty acid component of both neutral and polar lipids, especially saturated fatty acids, have high thermal stability,[31,32] some of the other hydrolysis products (*e.g.*, glycerol, phosphoric acid[33]) are subject to degradation at elevated temperatures.[7,33] Hence, species with higher fatty acid-to-total lipid ratio are expected to have higher conversion efficiency to the non-polar biocrude product.[34,35] The feedstocks used in this study have much lower fatty acid-to-total lipid ratios than the algal species used by Leow *et al.* (63.0±16.3% in this study versus 75.8±10.8% in Leow *et al.*, both for unmodified species),[4] consistent with the lower conversion coefficient observed here.

According to the MCA model parameters, aqueous co-products (measured as TDS) derive almost exclusively from protein and ash components in the biomass feedstock. Contributions of the former result in a large (45.9±14.9%) partitioning of nitrogen to the aqueous co-product, agreeing with results obtained from HTL of model proteins.[12] A large ash-to-aqueous conversion coefficient (0.86) was obtained, but contributions from protein still dominate due to the much lower ash contents in the microalgae feedstocks (11.4 – 69.8 dw% protein versus 2.0 – 13.1 dw% ash). The low ash contents also lead to relatively large uncertainties in ash-to-aqueous (±0.63) and ash-to-biochar (±0.43) conversion coefficients. These large uncertainties are also attributed to the fact that partitioning of ash components between aqueous and biochar co-products is likely to be influenced by the solubility of specific ionic components within the ash (*e.g.*, Na^+ versus Ca^{2+} cations; Cl^- versus PO_4^{3-} anions).

Whereas lipid, protein, and ash components contribute mainly to biocrude product and aqueous co-product, the conversion coefficients for the carbohydrate fraction reveal that this component is predominantly converted to gas (0.46) and biochar (0.41) co-products. Again, this finding is consistent with the general findings for HTL conversion of model carbohydrates,[12,36,37] where dehydration, decarboxylation (of organic acids from decomposition of monosaccharides[38]), polymerization, and solid-solid reactions of the carbohydrate hydrolysis products result in gas and biochar formation.[36,37,39] Enhanced occurrence of dehydration reactions from high carbohydrate feedstock is also consistent with the high carbon contents and black appearance of biochar formed from these species (Figure S3 in the ESI†). The ash-to-biochar conversion coefficient (0.18) also indicates that biochar contains ash component from the feedstock, possibly resulting from precipitation of common polyvalent cations (*e.g.*, Ca^{2+}, Mg^{2+}) present within biomass.[40,41]

2.2 Elemental composition of HTL products

Comprehensive HTL models need to predict not only multiphase HTL product yields, but also the chemical characteristics of the individual products. Leow *et al.* introduced preliminary methods for predicting carbon distribution to biocrude product and aqueous co-product (Figure S4 in the ESI†).[4] Here, predictions of more complete HTL product characteristics were built on this theme. Compositional analyses of products showed that elemental (C/H/N) contents of a particular HTL product were closely related to contents of feedstock components containing the same element, and were also major contributors to that particular product. As such, the same multiphase component additivity approach was applied (**Table 2**, **Figure 2**), and linear relationships were constructed as:

$$M_i = a \times J + b \quad (3)$$

where M_i is the weight percentage (wt%) of element M in product i, J is the identified feedstock descriptor variable (*e.g.*, feedstock protein content), a is the sensitivity coefficient, and b is the intercept (fixed at zero for most correlations).

View Article Online
DOI: 10.1039/C6GC03294J

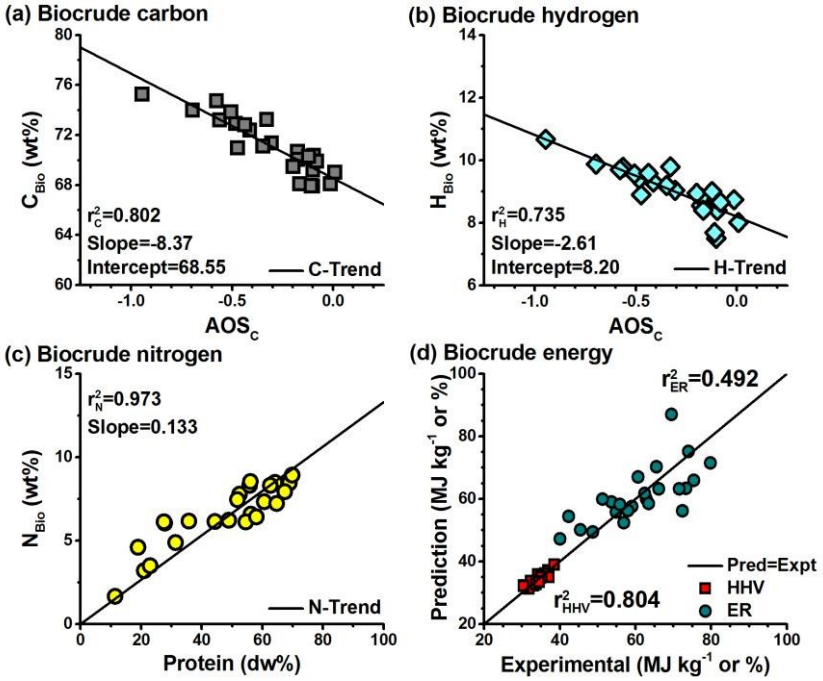

Figure 2 (a) to (c): observed linear relationships between biocrude elemental composition (C/H/N, wt%) and feedstock characteristic descriptor variables, data are from this study. (d): predicted versus experimental biocrude HHV (squares, MJ kg^{-1}) and ER (circles, %) results for calibration data (from this study), with r^2 values relative to the 1:1 correlation line. Detailed data are provided in Tables S1 and S2 in the ESI†.

Table 2 MCA model coefficients for HTL product characteristics[a]

Phase	M_i	J	a[c]	b
Biocrude	C_{Bio} (%)	AOS_C[b]	-8.37 (±1.84)	68.55 (±0.72)
	H_{Bio} (%)	AOS_C	-2.61 (±0.69)	8.20 (±0.27)
	N_{Bio} (%)	Prot%	0.133 (±0.010)	0[d]
Aqueous	TOC (mg L^{-1})	Prot%	478 (±37)	0[d]
	TN (mg L^{-1})	Prot%	251 (±19)	0[d]
Biochar	C_{Char}[e]	Carb%	1.75 (±0.24)	0[d]

[a] Coefficients and statistical characteristics calculated by the Regression program in Microsoft® Excel 2016 Analysis Toolpak. C_{Bio}, H_{Bio}, and N_{Bio} are wt% elemental contents of the biocrude product; C_{Char} is the wt% carbon content of the biochar. Statistical analysis results are listed in Table S6 in the ESI†.
[b] AOS_C calculated according to eq 4; Prot% and Carb% are the measured protein and carbohydrate contents (dw%) in the feedstock, respectively.
[c] Uncertainties provided at the 95% confidence level.
[d] Correlation intercept fixed at zero.
[e] Expression applicable for Carb% <37% (C_{Char} <65 wt%), biochar carbon content is expected to remain constant at 65 wt% for Carb% ≥37%.

It is revealed that biocrude carbon content (C_{Bio}, wt%) and hydrogen content (H_{Bio}, wt%) are correlated with the average oxidation state of feedstock carbon (AOS_C; **Figure 2a – b**; Table S1 in the ESI†), with AOS_C estimated as:[42]

$$AOS_C = \frac{(3\times \text{N mol\%} + 2\times \text{O mol\%} - \text{H mol\%})}{\text{C mol\%}} \quad (4)$$

where C/H/N/O mol% are the molar contents of corresponding elements in feedstock.

This correlation is consistent with observations that feedstocks with higher C and H contents and lower O contents (*i.e.*, more negative AOS_C) tend to yield biocrudes with higher C and H contents. The correlations are rationalized by the fact that characteristic AOS_C values for lipids < proteins < carbohydrates, so the overall feedstock AOS_C will increase (*i.e.*, become less negative) as biochemical composition shifts from lipid- to protein- to carbohydrate-dominant compositions (example calculation in Section S3 in the ESI†).

Biocrude nitrogen content (N_{Bio}, wt%) was found to correlate well with feedstock protein content (Prot%, as dw%; **Figure 2c**), a result of the fact that proteins are the dominant source of nitrogen in microalgae cells. Since a nitrogen-to-protein conversion factor of 6.25 is used in this study during feedstock characterization (Section S5 in the ESI†), the correlation suggests that biocrude nitrogen contents are 83.1±6.25% of the feedstock nitrogen contents, consistent with previous literature (72.6±19.4%).[4] Although not explicitly shown, it follows that biocrude oxygen content (O_{Bio}, wt%) can then be estimated by mass balance closure together with the predicted C_{Bio}, H_{Bio}, and N_{Bio} values. Examined and supported by our calibration dataset (Figure S7a in the ESI†), the established correlations are demonstrated to be accurate.

Combining the MCA-derived equations for biocrude elemental composition (eq 3 and **Table 2**) with Dulong's equation for estimation of fuel higher heating value (HHV, eq S3[43] in the ESI†) allows us to predict the HHV of biocrude (HHV_{Bio},

View Article Online
DOI: 10.1039/C6GC03294J

MJ kg^{-1}) directly from the feedstock's AOSc value and protein content as:

$$HHV_{Bio} = 30.74 - 8.52 \times AOS_C + 0.024 \times Prot\% \quad (5)$$

Biocrude energy recovery (ER, %), the percentage of the feedstock's inherent energy content recovered in the biocrude product, can also be predicted by combining the MCA model predictions for biocrude yields (Y_{Bio}, eq 2 and **Table 1**), HHV_{Bio} (eq 5), and feedstock HHV (HHV_{Feed}, calculated from feedstock elemental composition by eq S3[43] in the ESI†):

$$ER = \frac{(0.85 \times Lip\% + 0.45 \times Prot\% + 0.22 \times Carb\%) \times HHV_{Bio}}{HHV_{Feed}} \times 100\% \quad (6)$$

where Lip%, Prot%, and Carb% are dw% contents of feedstock lipid, protein, and carbohydrate components.

Strong agreements between HHV predictions and measurements demonstrates that the model can accurately predict the quality of biocrude products (**Figure 2d**, Figure S7a in the ESI†). The r^2 value for ER predictions drops to 0.492 because of a single data point that is greatly over-predicted (**Figure 2d**), which is a combined result of over-predicted biocrude yield and HHV value. However, 87.5% of the predictions are within ±10% of the experimental results, which suggests that although the MCA model was empirically derived from observed trends, it is capable of providing crucial information on biocrude product quality and evaluating associated energy recovery.

Unlike the biocrude product – which is simultaneously influenced by feedstock lipid, protein, and carbohydrate contents – the MCA model indicates that the non-ash fraction of the aqueous co-product is derived almost exclusively from feedstock protein component (**Table 1**). Therefore, predicting elemental composition of the volatile fraction of aqueous co-product is more straightforward. Both total organic carbon (TOC, mg L^{-1}) and total nitrogen (TN, mg L^{-1}) contents of the aqueous co-product correlate with feedstock protein content (**Figure 3a – b**), and the predictions are shown to be quite accurate (Figure S7b in the ESI†). Besides TOC and TN, the ratio of NH_4^+-N/TN can also be connected to feedstock protein content when Prot% <40% (NH_4^+-N/TN <51%, Figure S5 in the ESI†). However, for Prot% ≥40%, most of the ratios remain between 40 – 60%, but two of them are larger than 70%, and are not well correlated with Prot% (Figure S5 in the ESI†). Both of these trends have been previously reported,[4,44] but the rationale for such variations remains unclear. Therefore, additional investigation for factors controlling aqueous nitrogen speciation is warranted to further optimize nutrient recycling within HTL biorefineries and associated feedstock cultivation processes.

As gas co-product has been widely believed to be predominantly CO_2,[45–47] which is the product of the reported major deoxygenation mechanism for carbohydrates,[48,49] gas co-product composition was not characterized here. Following the same principle in predicting elemental composition of biocrude/aqueous products, carbon content of the biochar co-product (C_{Char}, wt%) was found to best correlate with

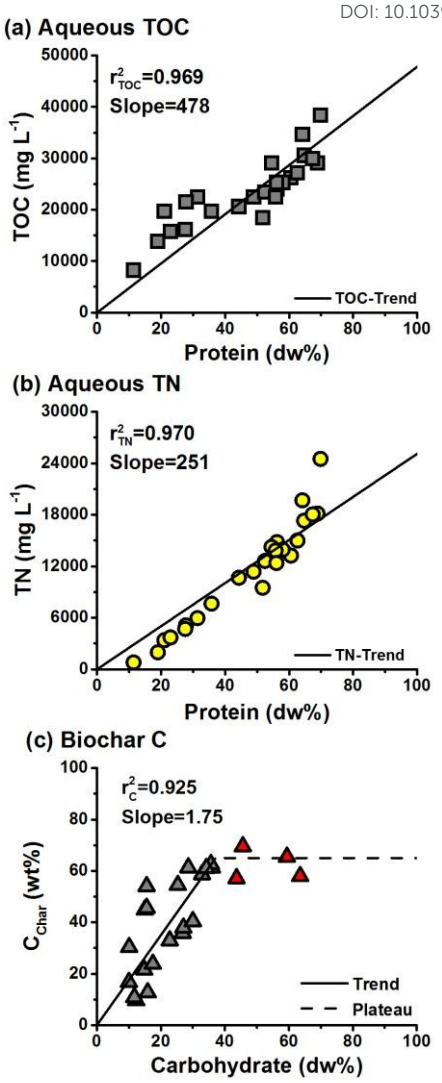

Figure 3 Linear relationship between feedstock and HTL co-product properties. Plot (a) is the observed trend between aqueous TOC (mg L^{-1}) and feedstock protein content (dw%). Plot (b) is the observed trend between aqueous TN (mg L^{-1}) and feedstock protein content. Plot (c) is the observed trend between biochar carbon content (wt%) and feedstock carbohydrate content (dw%), with the solid line showing the linear trend for C_{Char} up to the maximum (dashed line, C_{Char} of 65 wt% at 37 dw% feedstock carbohydrate content). All data are from this study, and detailed data are provided in Tables S1 and S2 in the ESI†.

feedstock carbohydrate content (Carb%, dry weight basis, **Figure 3c**). This is consistent with yield predictions suggesting carbohydrate to be the only contributor to biochar formation other than ash (**Table 1**). However, it was found that for feedstock species with Carb% ≥37 dw%, the carbon content of biochar reached a plateau of 65 wt% (red triangles in **Figure 3c**). This finding is consistent with previous work on hydrothermal production of carbonaceous materials, where C_{Char} values of 60 – 70 wt% were reported for pure carbohydrate model compounds (glucose, sucrose, starch, and xylose).[50] Thus, it is concluded that C_{Char} will increase proportionally with feedstock carbohydrate content (solid line in **Figure 3c**) until it reaches a maximum value representative of pure carbohydrate

feedstocks (C_{Char} of 65 wt% at 37 dw% feedstock carbohydrate content), then C_{char} will remain constant at 65 wt% for feedstocks with carbohydrate contents greater than 37 dw% (dashed line in **Figure 3c**). Predictions are generally acceptable with a r^2 of 0.661 for the calibration dataset (Figure S7b in the ESI†), but the discrepancies are larger compared to predictions for biocrude product and aqueous co-product, which are attributed, in part, to the relatively low yields of biochar and difficulties in recovering these small amounts of biochar during the experiments. Similar to C_{Char}, a correlation between feedstock carbohydrate content and biochar hydrogen content (H_{Char}, wt%) was anticipated, but no relationship was apparent (Figure S6a in the ESI†). Meanwhile, based on the MCA model, the protein component does not contribute significantly to biochar formation, so minimal nitrogen content was expected in the biochar. However, elemental analysis of biochar samples show that N_{Char} can be as high as 5.6 wt%, and the value appears to increase with feedstock carbohydrate content (Figure S6b in the ESI†). The trend could come from a carbohydrate-related "trap" effect associated with the unmixed minitube reactors used in this study: when carbohydrates are carbonized (due to insufficient access to water), the generated biochar can encapsulate or adsorb some protein (because of its adsorptive ability[51–54]). Thus, lower N_{Char} values are expected for the same feedstocks processed in larger continuous flow reactors where feedstocks are more evenly mixed with water. Additionally, Maillard reaction between hydrolysis products of proteins (amino acids) and carbohydrates (sugars) could yield nitrogen-containing re-polymerization products that end up in the biochar product.[55] Therefore, N_{char} could be affected by both protein and carbohydrate components in the feedstock, but the influence could not be accurately quantified at this time. It follows that no attempt was made to develop predictive correlations for H_{Char} and N_{Char} at this time.

2.3 Model validation and outlook

2.3.1 Biocrude product predictions and energy recovery. Being the main product of HTL and upgradable to fungible transportation fuels, the biocrude product is of the greatest interest to researchers and technology developers. Hence, validation was first performed for biocrude yield predictions using all available literature data reported for HTL of microalgae feedstocks carried out at 300 °C for 30 min reaction time (**Figure 4a**, filled symbols). The MCA model provides satisfying predictions even across literature yields that have a wider and higher range of biocrude yields (28.0 – 68.3 dw% from literature versus 21.3 – 54.3 dw% in this study). Predictions are comparably accurate with average residuals being only 3.7 dw% (literature) and 2.3 dw% (this study). In addition, the r^2 value for literature dataset (0.884) is even larger than that obtained with the internal calibration data set (0.718). This suggests that the model can provide reliable predictions of biocrude yield for a wide range of microalgae feedstocks measured in different experimental setups (*e.g.*, unmixed minitube reactors,[4] autoclaves,[47] large volume stirred reactors[18,28,29,46,56–61]).

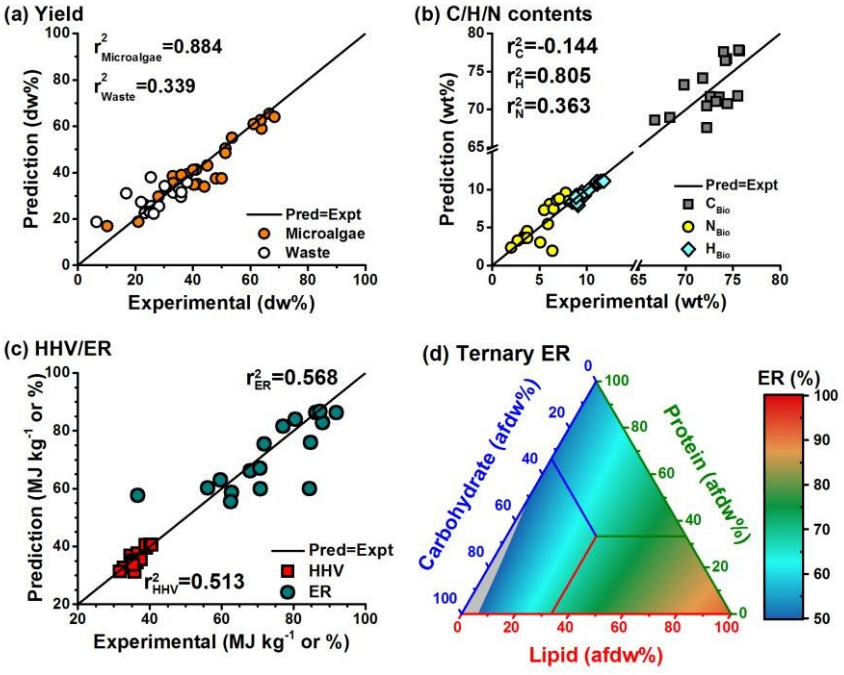

Figure 4 MCA predicted versus experimental results for biocrude yields and properties. All data in (a) – (c) are from literature (HTL conducted at 300 °C for 30 min for microalgae, 300 °C for 0 – 60 min for waste biosolids), with r^2 values relative to the 1:1 correlation line. Plot (a) is for predictions for biocrude yields for literature data, with either microalgae (filled symbols) or waste biosolids (open symbols) as feedstocks. Plot (b) is for predictions for biocrude C/H/N contents for literature data, with only microalgae as feedstock due to the scarcity of characterization data from waste biosolids. Plot (c) is for predictions for biocrude energetic parameters predicted by the MCA model (eqs 3, 5, and 6) using yields predicted in plot (a) and biocrude C/H/N contents predicted in plot (b) (only literature data with microalgae as feedstock were included). Plot (d) illustrates the biocrude ER for varying biochemical composition using an average elemental composition of lipids ($C_{57}H_{104}O_6$), proteins ($C_6H_{13.1}O_1N_{0.6}$), and carbohydrates ($(C_6H_{10}O_5)_n$).[62] Gray area indicates ER <50%.

Mixed feed processing has been proposed for HTL to eliminate effects of seasonal variation in algal productivity and improve process economics,[10] and co-processing of waste biosolids with algal biomass has been identified as a strategy for improving system stability, energy production, and nutrient recovery.[22] Thus, biocrude yield predictions were also compared with reported measurements of biocrude produced from 15 batches of different waste biosolids, including anaerobic sludge,[19] sewage sludge,[20,21] and swine manure[19,22] under HTL conditions of 300 °C (**Figure 4a**, open symbols). Due to the scarcity of available literature that include appropriate feedstock characterization data, reports with a reaction time of 0 – 60 min were included. The model generally provides accurate predictions except for three over-predicted points, which we speculate may be due to insufficient reaction time for HTL conversion of waste biosolids: feedstock biochemical composition for two data points (entries 11 and 12, Table S8 in the ESI†) are almost identical, but biocrude yield for the sample with a 60-minute reaction time is much closer to the predicted value (38 dw% experimental versus 36 dw% predicted) than the sample with a 30-minute reaction time (25 dw% experimental versus 38 dw% predicted). Further research is needed to examine this issue, which may be critical for efforts to valorize waste biosolids *via* HTL. Regardless, the model is shown to be generally effective for waste biosolids, pushing the boundary of the MCA model from microalgae feedstocks alone to a wider range including waste biosolids.

Predictions for biocrude C/H/N contents were also evaluated with literature data, but only microalgae feedstocks were included since few studies on HTL of waste biosolids have provided such characterization data. Hydrogen content is the most accurately predicted, while further improvements can be made for carbon and nitrogen contents (**Figure 4b**). Though the r^2 value for carbon content is comparably much lower, the maximum absolute error is only 4.6 wt%, or 6.4% of the experimental value. Predictions for nitrogen content are greatly affected by two data points that are significantly under-predicted, which may be a result of the uniform 6.25 nitrogen-to-protein conversion factor[63] assumed for this study. Though the factor of 6.25 has been suggested to be an appropriate estimation for most plant and animal proteins,[63] previous studies have shown that this conversion factor is subject to change due to variations in algae species and cultivation conditions.[64,65] Observed trends are expected to hold true across algal species, but future applications of the model should leverage species- and cultivation-specific nitrogen-to-protein conversion factors when such information is available. Alternatively, direct measurements of feedstock protein content could replace the use of this conversion factor, but would require more complicated methods and specialized equipment not readily available to many users of the model and still might not provide improved accuracy.[64] Nevertheless, the model does relatively well considering the variability in reactor setup and product recovery/characterization protocols used in the different literature studies.

With predictions for both product yields (eq 2) and elemental composition (eq 3), HHV and ER values for the biocrude product were then calculated (eqs 5 and 6) and compared to results calculated directly from experimental measurements. With the exception of one or two points showing larger deviation, the predictions are generally robust (**Figure 4c**). **Figure 4c** also shows the predicted biocrude ER for feedstocks representing the full biochemical compositional space (calculated assuming average elemental compositions of lipids as $C_{57}H_{104}O_6$, proteins as $C_6H_{13.1}O_1N_{0.6}$, and carbohydrates as $(C_6H_{10}O_5)_n$[62]). The resulting biocrude ER map supports previous findings that high lipid feedstocks (bottom right) not only produce higher biocrude yields, but the products are of higher quality (*i.e.*, higher C and H contents, lower N and O contents, and thus higher HHV). ER of high protein species (top) are comparably lower, but these species still retain the potential for being good feedstock options because of their faster growth rates and lower cultivation costs,[2,4,66] especially compared to high lipid species.[2,67,68] Since a substantial part of the feedstock energy will be diverted to aqueous co-product, proper management of aqueous co-product is required for high protein species. In the case of high carbohydrate content feedstocks (bottom left), most of the inherent energy will be converted to gas (predominantly CO_2[46,47,49]) or biochar co-products, and biocrude ER from direct HTL of such species is predicted to be low. Thus, biorefinery processing should be modified to provide a more effective valorization pathway for the carbohydrate fraction in algal biomass. For example, dilute acid digestion of feedstocks followed by fermentation of the resulting sugar stream to ethanol prior to HTL processing may provide extra fuel revenue.[66,69]

2.3.2 Co-product predictions. Due to the lower yields, co-products are often overlooked and fewer reports have quantified their formation or characteristics. In addition, recoveries of co-products are highly dependent on experimental procedures, so larger discrepancies between model predictions and co-product yields reported in literature are expected and observed (**Figure 5a**). Predictions for biochar co-product yields are comparably better with points generally laying along the 1:1 line. Aqueous yield measurements reported in the literature are generally under-predicted, most likely due to different methods used for yield quantification (*e.g.*, time and temperature used for TDS determination, which were not specified in some studies[27,56]). Studies in which aqueous product yields were estimated by mass balance closure were omitted from the model analysis. According to the model, gas yields were predicted to fall between 10 – 15 dw%, while the experimental values covered a wider range (9 – 22 dw%), revealing the model is not sensitive enough towards gas yields, and predictions are often smaller than actual values. Though yields of aqueous co-product are not accurately predicted, predictions of TOC and TN contents are considerably accurate (**Figure 5b**, left and bottom axes). The r^2 values for both TOC (0.785) and TN (0.921) exceed the calibration values (0.568 for TOC, and 0.862 for TN), supporting application of the model as a valuable tool in providing guidance for aqueous co-product utilization. For carbon content of biochar co-product, predictions are generally lower than experimental results reported, especially towards the higher end (*i.e.*, more carbonaceous biochars with less influence from ash component,

View Article Online
DOI: 10.1039/C6GC03294J

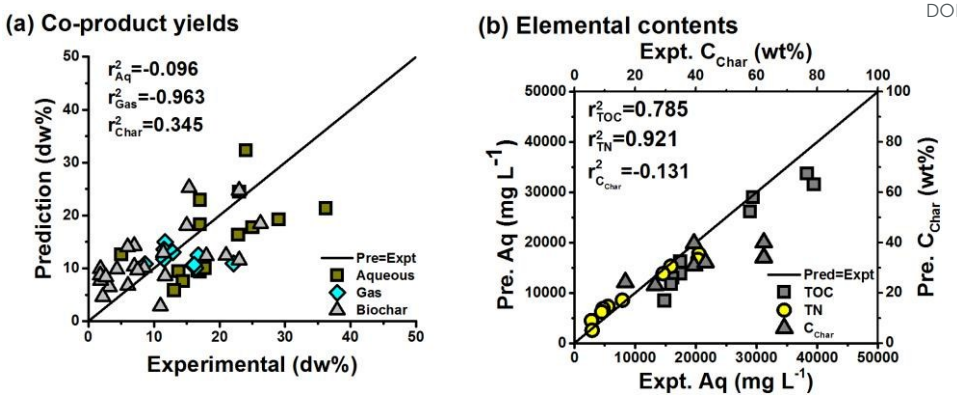

Figure 5 MCA predicted versus experimental results for (a) co-product yields; and (b) co-product elemental composition, left and bottom axes are for aqueous TOC/TN contents while right and top axes are for biochar carbon content. All data are from literature with microalgae as feedstock (HTL conducted at 300 °C for 30 min), and r^2 values are relative to the 1:1 lines. Detailed data are provided in Tables S7 and S9 in the ESI†.

Figure 5b, right and top axes). This is expected to be a result of the very low biochar yields (<5 dw%) reported in literature. Artifacts resulting from product recovery and analysis of such small amounts of biochar (*e.g.*, filter fibers could be scratched off and mixed with biochar) could have disproportionately large impacts on the resulting C_{Char} measurements.

For co-products in general, the MCA model can accurately predict aqueous characteristics (TOC and TN contents), but the other predictions will benefit from additional research leveraging harmonized protocols among investigators for co-product recovery, quantification, and characterization.

2.3.3 Research needs towards integrated modeling frameworks. The last few years have witnessed significant progress in compositional based HTL predictive models: accuracy of the biocrude component additivity models has been greatly improved (Figure S9a – b in the ESI†), but further improvements are still required for predicting biocrude composition (Figure S9c – d in the ESI†) as well as yields and characteristics of HTL co-products. The MCA model introduced here is able to provide reliable predictions for both yields and characteristics of HTL products, all based upon commonly measured properties of the microalgae feedstock. However, differences in reactor setup and experimental procedures across the literature has led to deviations in predictions, especially for co-products. In this study, experiments were conducted in unmixed batch reactors, leading to generally unclosed product mass balances (80.6±7.5 dw%), and the lost mass may stem from non-FA fraction of lipid and protein components (Figure S10 in the ESI†). Hence, the sum of the conversion coefficients for all HTL products for lipid (0.85) and protein (0.76) components are smaller than unity. Since quantification of both biocrude and aqueous products involves evaporation steps, the lost mass is likely to be associated with small-molecule compounds that are volatilized during these procedures. Similar mass balance discrepancies during HTL processing have been reported previously,[70,71] with some studies categorizing the unaccounted-for mass as a "volatile" fraction.[17] The lost mass may include water molecules[36,37,72] and other volatile inorganic (*e.g.*, dissolved CO_2[48]) or organic (*e.g.*, volatile fatty acids[73]) compounds dissolved in the biocrude or aqueous products. Lipid- and protein-involving reactions like deamination, decarboxylation,[58,74] Maillard reactions,[55] and polymerization reactions[58] – products of which have been widely detected in biocrude and aqueous products[19,58,75] – could yield low molecular weight volatile compounds that are lost during evaporative recovery steps. To enhance reaction efficiency and product recovery, real world applications of HTL are likely to employ different reactor setups (*e.g.*, continuous flow reactor instead of batch reactor) and procedures (*e.g.*, physical separation of products instead of solvent recovery).[10] Therefore, further research with such experimental setups and procedures are necessary to assess and validate the MCA model to reconcile these differences. Regardless, the structure and correlations proposed in the MCA model should be applicable and only fine-tuning of some coefficients is anticipated. Additionally, interactions between feedstock components (*e.g.*, Maillard reaction between amino acids and sugars,[76,77] amide-forming reaction between fatty acids and amino acids[43,78,79]) have been observed in previous studies, which may be responsible for some of the deviations between model predictions and experimental results. This may be particularly true for co-products, as previous work has suggested interactions between feedstock components only have a small effect on biocrude product yields,[12] and the MCA model predictions are generally robust for biocrude, while less accurate for the co-products. Further research is needed to evaluate the influence of cross-component reactions on yields and properties of HTL co-products and incorporate such reactions within predictive models.

3 Conclusions

To date, considerable efforts have been made to assess HTL as a potential technique for biofuel production.[9,10,19,22,45,80] However, published studies were typically based on experimental results from a limited number of feedstocks, neglecting the fact that differences in feedstock properties could significantly shift the product distribution, and properties of microalgae species could be greatly impacted by cultivation

decisions.[81,82] According to data collected in this study, biocrude yields can be as low as 21.3 dw% or as high as 68.3 dw%, which is impactful given a previous report has suggested that a 20% decrease in the biocrude oil yield could result in a 14% increase in MFSP.[10] Therefore, the lack of ability to reflect such compositional diversity undermines the ability of previously published studies by failing to note the wide range of biofuel production costs from wide breadth of feedstocks available. Meanwhile, proper management of co-products is required to maximize energy and nutrient recovery,[10,83–85] as the aqueous co-product alone can represent up to 40% of the HTL yields, 20% of the feedstock carbon, and 60% of the nitrogen,[10] and biochar co-product is also an important energy/nutrient source.[86] Several techniques have been developed to harvest the energy in aqueous co-product, including anaerobic digestion (AD)[80] and catalytic hydrothermal gasification (CHG).[45] However, optimization in these processes has been limited by the lack of quantitative understanding of the aqueous co-product for proper management. Moreover, it has also been pointed out that the life cycle environmental impacts of algae cultivation are driven by the large demand of CO_2 and fertilizers,[87] which can be reduced by recycling HTL co-products.[10,18] Therefore, models with the predictive power towards yields and characteristics of HTL biocrude product as well as co-products must be incorporated for more resilient studies.

In this contribution, results from HTL experiments (300 °C, 30 min) conducted with 24 batches of microalgae feedstocks of varying biochemical and elemental compositions were used to inform the development of a multiphase component additivity (MCA) model. The MCA model provides insight into the close correlations between feedstock and both yields and characteristics of all HTL products. Additionally, a combination of yields and characteristics predictions enables us to examine energy and nutrient flows from feedstock to products, and understand the energy/nutrient distribution between products. Moreover, the model retains the merit of simplicity in earlier feedstock component additivity models while improving upon predictive accuracy.

Consequently, introduction of the MCA model provides a comprehensive tool for designing and evaluating HTL-integrated biorefinery or valorization systems for waste biosolids. For instance, when combined with upstream cultivation models,[81,82] a complete modeling system could be constructed to predict HTL outcomes for a particular microalga cultivated from a set of specific operational decisions, allowing downstream conversion plants to be customized to meet the needs for that species, and the simulation of varied cultivation conditions would allow operators to optimize cultivation and conversion schemes. This is also applicable for waste stream valorization. Previous studies have promoted the scheme of using urban wastewater to cultivate microalgae, then applying HTL for biofuel production and nutrient recovery.[86] With the MCA model, flow of energy and nutrients within the system could be tracked, aiding the development of integrated processes with multi-targets of waste treatment, energy production, and nutrient recovery. Even for waste streams like sludge and manure which cannot be used for microalgae cultivation, the model could be used to compare the recovery efficiency between HTL and other conventional techniques (*e.g.*, AD), enabling us to examine the pros and cons of different valorization methods.

In conclusion, incorporation of the MCA model into process evaluation studies offers an opportunity to examine system performance with varying feedstock composition and provide guidance in developing composition-specific valorization pathways for different feedstocks, paving a path forward for economically feasible and environmentally sustainable biofuels.

4 Methods

4.1 Biochemical diversity of HTL feedstocks

A total of 24 batches of biomass samples with 0 – 46.7 afdw% (ash free dry weight basis) lipids, 12.9 – 85.6 afdw% proteins, and 12.8 – 75.8 afdw% carbohydrates were used as HTL feedstocks for model calibration (Figure S1, Table S1 in the ESI†). Details of microalgae acquisition and characterization are provided in Section S5 in the ESI†. The feedstock collection included 12 batches of microalgae from *Chlorella* (CZ), *Scenedesmus* (SD), *Chlorogloeopsis* (Cf), and *Spirulina* (Sp) species and defatted (*i.e.*, lipid-extracted) biomass obtained from each batch. Protein was the dominant component for most batches, except for subsets of high lipid and/or high carbohydrate batches of *Chlorella* and *Scenedesmus*. Elemental analysis revealed that carbon was the most abundant element, ranging from 42.7 to 56.9 dw%. Hydrogen content varied over a narrow range from 6.1 – 8.7 dw%, whereas nitrogen content ranged from as low as 1.8 dw% to as high as 11.2 dw%. Oxygen content was calculated by difference (100 – ash% – C% – H% – N%) and varied from 23.5 to 43.5 dw%. Most importantly for the current effort, is that the wide-ranging feedstock composition reduced bias in model calibration resulting from either domination of a particular component or small variations in any single component.

4.2 Other experimental methods

HTL reaction and product recovery followed the same procedures as previously reported.[4] Most of the product analyses also followed the same protocols as reported.[4] Details about experimental methods can be found in Section S5 in the ESI†.

4.3 Model calibration and validation

The MCA model for product yields (eq 2) with 16 conversion coefficients k_{ij} (4 components contributing to 4 different products) was calibrated in two stages: First, conversion coefficients for each product were determined individually by least-squares fitting to measured data, and the coefficients were constrained to be non-negative and smaller than 1. For each product, 24 data points were used for 4 coefficients, which is so far the largest data-to-coefficient ratio among all HTL modeling work. Then, coefficients which were found to be smaller than 0.10 with large p-values (>0.05) were excluded from the model formulation (*i.e.*, set to 0) because the null hypothesis (*i.e.*, $k_{ij} = 0$) could not be rejected (gray cells in Table

S5 in the ESI†). These statistics-derived exclusions are all consistent with HTL results reported for model lipid, protein, and carbohydrate reference compounds,[12] and exclusion of ash (mostly inorganic salts associated with the algal biomass) contributions to both gas and non-polar biocrude products is reasonable. In the second stage, the remaining 9 coefficients were re-fit to obtain the final coefficients (**Table 1**, Table S5 in the ESI†).

For products' elemental composition, correlation coefficients (a and b in eq 3) were obtained by least-squares fitting to measured data (24 data points for each correlation, **Table 2**). Consistent with the large r^2 values, the very low p-values and significance F values (Table S6 in the ESI†) validated these correlations to be statistical significant.

The calibrated model expressions were externally validated by comparison with all measured values reported in the literature where HTL experiments were performed at 300 °C and feedstock biochemical compositions were reported. For product yields, only data that were directly measured (as opposed to being estimated by difference to close the mass balance) were included in model validation. For microalgae feedstocks, only data for 30 min reactions were used for validation, but data from 0 – 60 min reaction time were included for validation of biocrude yields from waste biosolids due to the scarcity of such data. The microalgae-based validation dataset consisted of results from 13 studies involving 25 different batches of microalgae, including freshwater species,[46,56–58,60,61] marine species,[4,27,46,47,56,59] defatted (lipid-extracted) batches,[4,27] harvested mixed batches,[18,29] and a wild mixed batch.[28] For waste biosolids, 4 studies with 15 different feedstocks were included, containing anaerobic sludge,[19] sewage sludge,[20,21] swine manure,[19,22] and mixed wastewater algae and swine manure.[22] The large dataset is currently the most diverse in HTL modeling, and is the only one that contains both microalgae and waste biosolids as feedstocks.

Acknowledgements

Financial support was provided by National Science Foundation (NSF) through the NSF Engineering Research Center for Re-inventing the Nation's Urban Water Infrastructure (ReNUWIt; EEC-1028968) and NSF awards CBET-1555549 and CBET-1438667. S. Leow is supported by the National Research Foundation (NRF) Singapore under its NRF Environmental and Water Technologies (EWT) PhD Scholarship Programme and administered by the Environment and Water Industry Programme Office (EWI). Tao Dong, Lieve Laurens, Nicholas Nagle, and Philip Pienkos (National Renewable Energy Laboratory) are acknowledged for supply of selected feedstocks and helpful discussion and feedback. Patrick Biller (Aarhus University) is acknowledged for supply of selected feedstocks. John Scott and Susan Barta (UIUC, ISTC) are acknowledged for providing analytical support.

References

1 U.S. Department of, *National Algal Biofuels Technology Roadmap*, US Department of Energy, Office of Energy Efficiency and Renewable Energy, Biomass Program, Washington, D.C., WA, 2010.
2 P. J. le B. Williams and L. M. L. Laurens, *Energy Environ. Sci.*, 2010, **3**, 554–590.
3 P. M. Foley, E. S. Beach and J. B. Zimmerman, *Green Chem.*, 2011, **13**, 1399–1405.
4 S. Leow, J. R. Witter, D. R. Vardon, B. K. Sharma, J. S. Guest and T. J. Strathmann, *Green Chem*, 2015, **17**, 3584–3599.
5 A. A. Peterson, F. Vogel, R. P. Lachance, M. Fröling, M. J. Antal Jr. and J. W. Tester, *Energy Environ. Sci.*, 2008, **1**, 32–65.
6 Y. Zhang, in *Biofuels from Agricultural Wastes and Byproducts*, Wiley-Blackwell, 2010, pp. 201–232.
7 D. López Barreiro, W. Prins, F. Ronsse and W. Brilman, *Biomass Bioenergy*, 2013, **53**, 113–127.
8 D. C. Elliott, B. Patrick, A. B. Ross, A. J. Schmidt and S. B. Jones, *Bioresour. Technol.*, 2014, **178**, 147–156.
9 X. Liu, B. Saydah, P. Eranki, L. M. Colosi, B. Greg Mitchell, J. Rhodes and A. F. Clarens, *Bioresour. Technol.*, 2013, **148**, 163–171.
10 S. B. Jones, Y. Zhu, D. B. Anderson, R. T. Hallen, D. C. Elliott, A. J. Schmidt, K. O. Albrecht, T. R. Hart, M. G. Butcher, C. Drennan, L. J. Snowden-Swan, R. Davis and C. Kinchin, *Process Design and Economics for the Conversion of Algal Biomass to Hydrocarbons: Whole Algae Hydrothermal Liquefaction and Upgrading*, Pacific Northwest National Laboratory (PNNL), Richland, WA (US), 2014.
11 P. Biller and A. B. Ross, *Bioresour. Technol.*, 2011, **102**, 215–225.
12 G. Teri, L. Luo and P. E. Savage, *Energy Fuels*, 2014, **28**, 7501–7509.
13 P. J. Valdez, M. C. Nelson, H. Y. Wang, X. N. Lin and P. E. Savage, *Biomass Bioenergy*, 2012, **46**, 317–331.
14 P. J. Valdez and P. E. Savage, *Algal Res.*, 2013, **2**, 416–425.
15 P. J. Valdez, V. J. Tocco and P. E. Savage, *Bioresour. Technol.*, 2014, **163**, 123–127.
16 J. L. Faeth and P. E. Savage, *Bioresour. Technol.*, 2016, **206**, 290–293.
17 D. C. Hietala, J. L. Faeth and P. E. Savage, *Bioresour. Technol.*, 2016, **214**, 102–111.
18 Y. Zhou, L. Schideman, G. Yu and Y. Zhang, *Energy Environ. Sci.*, 2013, **6**, 3765–3779.
19 D. R. Vardon, B. K. Sharma, J. Scott, G. Yu, Z. Wang, L. Schideman, Y. Zhang and T. J. Strathmann, *Bioresour. Technol.*, 2011, **102**, 8295–303.
20 A. Suzuki, T. Nakamura, S.-Y. Yokoyama, T. Ogi and K. Koguchi, *J. Chem. Eng. Jpn.*, 1988, **21**, 288–293.
21 A. Suzuki, T. Nakamura and S. Yokoyama, *J. Chem. Eng. Jpn.*, 1990, **23**, 6–11.
22 W.-T. Chen, Y. Zhang, J. Zhang, L. Schideman, G. Yu, P. Zhang and M. Minarick, *Appl. Energy*, 2014, **128**, 209–216.
23 N. Beecher, K. Crawford, N. Goldstein, G. Kester, M. Lono-Batura and E. Dziezyk, *A National Biosolids Regulation, Quality, End Use & Disposal Survey*, Northeast biosolids and Residuals Associaton (NEBRA), Tamworth, NH, 2007.
24 J. Peccia and P. Westerhoff, *Environ. Sci. Technol.*, 2015, **49**, 8271–8276.
25 S. Xiu, A. Shahbazi, V. Shirley and D. Cheng, *J. Anal. Appl. Pyrolysis*, 2010, **88**, 73–79.
26 U.S. EIA, https://www.eia.gov/tools/faqs/faq.cfm?id=33&t=6, (accessed November 2016).
27 M. P. Caporgno, E. Clavero, C. Torras, J. Salvadó, O. Lepine, J. Pruvost, J. Legrand, J. Giralt and C. Bengoa, *ACS Sustain. Chem. Eng.*, 2016.
28 C. Tian, Z. Liu, Y. Zhang, B. Li, W. Cao, H. Lu, N. Duan, L. Zhang and T. Zhang, *Bioresour. Technol.*, 2015, **184**, 336–343.

29 W.-T. Chen, Y. Zhang, J. Zhang, G. Yu, L. C. Schideman, P. Zhang and M. Minarick, *Bioresour. Technol.*, 2014, **152**, 130–139.
30 J. Folch, M. Lees and G. H. Sloane Stanley, *J. Biol. Chem.*, 1957, **226**, 497–509.
31 T. Kocsisová, J. Juhasz and J. Cvengroš, *Eur. J. Lipid Sci. Technol.*, 2006, **108**, 652–658.
32 H.-Y. Shin, J.-H. Ryu, S.-Y. Park and S.-Y. Bae, *J. Anal. Appl. Pyrolysis*, 2012, **98**, 250–253.
33 S. M. Changi, J. L. Faeth, N. Mo and P. E. Savage, *Ind. Eng. Chem. Res.*, 2015, **54**, 11733–11758.
34 R. L. Holliday, J. W. King and G. R. List, *Ind. Eng. Chem. Res.*, 1997, **36**, 932–935.
35 J. W. King, R. L. Holliday and G. R. List, *Green Chem.*, 1999, **1**, 261–264.
36 Y. GAO, H. CHEN, J. WANG, T. SHI, H.-P. YANG and X.-H. WANG, *J. Fuel Chem. Technol.*, 2011, **39**, 893–900.
37 W. Shi, S. Li, J. Jia and Y. Zhao, *Ind. Eng. Chem. Res.*, 2013, **52**, 586–593.
38 M. Sevilla and A. B. Fuertes, *Chem. – Eur. J.*, 2009, **15**, 4195–4203.
39 A. Kruse, A. Funke and M.-M. Titirici, *Curr. Opin. Chem. Biol.*, 2013, **17**, 515–521.
40 C. Jazrawi, P. Biller, A. B. Ross, A. Montoya, T. Maschmeyer and B. S. Haynes, *Algal Res.*, 2013, **2**, 268–277.
41 N. Neveux, A. K. L. Yuen, C. Jazrawi, M. Magnusson, B. S. Haynes, A. F. Masters, A. Montoya, N. A. Paul, T. Maschmeyer and R. de Nys, *Bioresour. Technol.*, 2014, **155**, 334–341.
42 J. M. Dick, *J. R. Soc. Interface*, 2014, **11**, 20131095.
43 T. M. Brown, P. Duan and P. E. Savage, *Energy Fuels*, 2010, **24**, 3639–3646.
44 P. Biller, A. B. Ross, S. C. Skill, A. Lea-Langton, B. Balasundaram, C. Hall, R. Riley and C. A. Llewellyn, *Algal Res.*, 2012, **1**, 70–76.
45 D. C. Elliott, T. R. Hart, A. J. Schmidt, G. G. Neuenschwander, L. J. Rotness, M. V. Olarte, A. H. Zacher, K. O. Albrecht, R. T. Hallen and J. E. Holladay, *Algal Res.*, 2013, **2**, 445–454.
46 H. Li, Z. Liu, Y. Zhang, B. Li, H. Lu, N. Duan, M. Liu, Z. Zhu and B. Si, *Bioresour. Technol.*, 2014, **154**, 322–329.
47 L. Garcia Alba, C. Torri, C. Samorì, J. van der Spek, D. Fabbri, S. R. A. Kersten and D. W. F. (Wim) Brilman, *Energy Fuels*, 2012, **26**, 642–657.
48 S. M. Heilmann, H. T. Davis, L. R. Jader, P. A. Lefebvre, M. J. Sadowsky, F. J. Schendel, M. G. von Keitz and K. J. Valentas, *Biomass Bioenergy*, 2010, **34**, 875–882.
49 G. Yu, Y. Zhang, L. Schideman, T. Funk and Z. Wang, *Energy Environ. Sci.*, 2011, **4**, 4587–4595.
50 L. Yu, C. Falco, J. Weber, R. J. White, J. Y. Howe and M.-M. Titirici, *Langmuir*, 2012, **28**, 12373–12383.
51 B. Chen and Z. Chen, *Chemosphere*, 2009, **76**, 127–133.
52 G. James, D. A. Sabatini, C. T. Chiou, D. Rutherford, A. C. Scott and H. K. Karapanagioti, *Water Res.*, 2005, **39**, 549–558.
53 B. Chen and M. Yuan, *J. Soils Sediments*, 2010, **11**, 62–71.
54 M.-M. Titirici and M. Antonietti, *Chem. Soc. Rev.*, 2009, **39**, 103–116.
55 W. Yang, X. Li, Z. Li, C. Tong and L. Feng, *Bioresour. Technol.*, 2015, **196**, 99–108.
56 H. K. Reddy, T. Muppaneni, S. Ponnusamy, N. Sudasinghe, A. Pegallapati, T. Selvaratnam, M. Seger, B. Dungan, N. Nirmalakhandan, T. Schaub, F. O. Holguin, P. Lammers, W. Voorhies and S. Deng, *Appl. Energy*, 2016, **165**, 943–951.
57 C. Gai, Y. Zhang, W.-T. Chen, P. Zhang and Y. Dong, *RSC Adv.*, 2014, **4**, 16958–16967.
58 C. Gai, Y. Zhang, W.-T. Chen, P. Zhang and Y. Dong, *Energy Convers. Manag.*, 2015, **96**, 330–339.
59 J. Cheng, R. Huang, T. Yu, T. Li, J. Zhou and K. Cen, *Bioresour. Technol.*, 2014, **151**, 415–418.
60 D. R. Vardon, B. K. Sharma, G. V. Blazina, K. Rajagopalan and T. J. Strathmann, *Bioresour. Technol.*, 2012, **109**, 178–187.
61 W.-T. Chen, L. Tang, W. Qian, K. Scheppe, K. Nair, Z. Wu, C. Gai, P. Zhang and Y. Zhang, *ACS Sustain. Chem. Eng.*, 2016, **4**, 2182–2190.
62 B. Sialve, N. Bernet and O. Bernard, *Biotechnol. Adv.*, 2009, **27**, 409–416.
63 F. W. Sosulski and G. I. Imafidon, *J. Agric. Food Chem.*, 1990, **38**, 1351–1356.
64 L. M. L. Laurens, S. Van Wychen, J. P. McAllister, S. Arrowsmith, T. A. Dempster, J. McGowen and P. T. Pienkos, *Anal. Biochem.*, 2014, **452**, 86–95.
65 S. Lourenço, E. Barbarino, P. Lavín, U. Lanfer Marquez and E. Aidar, *Eur. J. Phycol.*, 2004, **39**, 17–32.
66 L. M. L. Laurens, N. Nagle, R. Davis, N. Sweeney, S. V. Wychen, A. Lowell and P. T. Pienkos, *Green Chem.*, 2015, **17**, 1145–1158.
67 T. M. Mata, A. A. Martins and N. S. Caetano, *Renew. Sustain. Energy Rev.*, 2010, **14**, 217–232.
68 L. Rodolfi, G. Chini Zittelli, N. Bassi, G. Padovani, N. Biondi, G. Bonini and M. R. Tredici, *Biotechnol. Bioeng.*, 2009, **102**, 100–112.
69 T. Dong, E. P. Knoshaug, R. Davis, L. M. L. Laurens, S. Van Wychen, P. T. Pienkos and N. Nagle, *Algal Res.*, 2016, **19**, 316–323.
70 D. López Barreiro, C. Zamalloa, N. Boon, W. Vyverman, F. Ronsse, W. Brilman and W. Prins, *Bioresour. Technol.*, 2013, **146**, 463–471.
71 J. Wagner, R. Bransgrove, T. A. Beacham, M. J. Allen, K. Meixner, B. Drosg, V. P. Ting and C. J. Chuck, *Bioresour. Technol.*, 2016, **207**, 166–174.
72 W. Abdelmoez, T. Nakahasi and H. Yoshida, *Ind. Eng. Chem. Res.*, 2007, **46**, 5286–5294.
73 M. Sevilla and A. B. Fuertes, *Carbon*, 2009, **47**, 2281–2289.
74 S. S. Toor, L. Rosendahl and A. Rudolf, *Energy*, 2011, **36**, 2328–2342.
75 M. Pham, L. Schideman, J. Scott, N. Rajagopalan and M. J. Plewa, *Environ. Sci. Technol.*, 2013, **47**, 2131–2138.
76 A. A. Peterson, R. P. Lachance and J. W. Tester, *Ind. Eng. Chem. Res.*, 2010, **49**, 2107–2117.
77 S. I. F. S. Martins, W. M. F. Jongen and M. A. J. S. van Boekel, *Trends Food Sci. Technol.*, 2000, **11**, 364–373.
78 S. Changi, M. Zhu and P. E. Savage, *ChemSusChem*, 2012, **5**, 1743–1757.
79 P. J. Valdez, J. G. Dickinson and P. E. Savage, *Energy Fuels*, 2011, **25**, 3235–3243.
80 B. Patel, M. Guo, C. Chong, S. H. M. Sarudin and K. Hellgardt, *Sci. Total Environ.*, 2016, **568**, 489–497.
81 J. S. Guest, M. C. M. van Loosdrecht, S. J. Skerlos and N. G. Love, *Environ. Sci. Technol.*, 2013, **47**, 3258–3267.
82 R. Davis, J. Markham, C. Kinchin, N. Grundl, E. C. D. Tan and D. Humbird, *Process Design and Economics for the Production of Algal Biomass: Algal Biomass Production in Open Pond Systems and Processing Through Dewatering for Downstream Conversion*, National Renewable Energy Laboratory (NREL), Golden, CO., 2016.
83 R. Davis, D. Fishman, E. D. Frank, M. S. Wigmosta, A. Aden, A. M. Coleman, P. T. Pienkos, R. J. Skaggs, E. R. Venteris and M. Q. Wang, *Renewable Diesel from Algal Lipids: An Integrated Baseline for Cost, Emissions, and Resource Potential from a Harmonized Model*, 2012.
84 R. Davis, C. Kinchin, J. Markham, E. Tan, L. M. L. Laurens, D. Sexton, D. Knorr, P. Schoen and J. Lukas, *Process Design and Economics for the Conversion of Algal Biomass to Biofuels: Algal Biomass Fractionation to Lipid- and Carbohydrate-Derived Fuel Products*, National Renewable Energy Laboratory (NREL), Golden, CO., 2014.
85 D. C. Elliott, T. R. Hart, G. G. Neuenschwander, L. J. Rotness, M. V. Olarte and A. H. Zacher, *Ind. Eng. Chem. Res.*, 2012, **51**, 10768–10777.

View Article Online
DOI: 10.1039/C6GC03294J

86 T. Selvaratnam, S. M. Henkanatte-Gedera, T. Muppaneni, N. Nirmalakhandan, S. Deng and P. J. Lammers, *Energy*, 2016, **104**, 16–23.
87 A. F. Clarens, E. P. Resurreccion, M. A. White and L. M. Colosi, *Environ. Sci. Technol.*, 2010, **44**, 1813–1819.

View Article Online
DOI: 10.1039/C6GC03294J

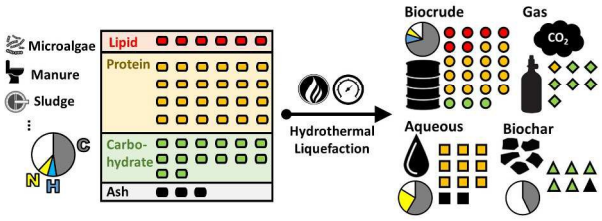

A multiphase component additivity (MCA) model to quantitatively predict both yields and characteristics of products from hydrothermal liquefaction of microalgae.